Understanding the negative effects of alkalis on long-term strength of Portland cement

Journal Article

Author(s):
Zhang, Mai; Zunino, Franco; Lu, Yang; Wang, Fazhou; Scrivener, Karen

Publication date:
2023-12

Permanent link:
https://doi.org/10.3929/ethz-b-000642262

Originally published in:
Cement and Concrete Research 174, https://doi.org/10.1016/j.cemconres.2023.107348

Cement and Concrete Research 174 (2023) 107348

Contents lists available at ScienceDirect

Cement and Concrete Research

journal homepage: www.elsevier.com/locate/cemconres

Understanding the negative effects of alkalis on long-term strength of Portland cement

Mai Zhang [a,b,c], Franco Zunino [c,*], Lu Yang [a,b], Fazhou Wang [a,b,**], Karen Scrivener [c]

[a] State Key Laboratory of Silicate Materials for Architectures, Wuhan University of Technology, 430070 Wuhan, China
[b] School of Materials Science and Engineering, Wuhan University of Technology, 430070 Wuhan, China
[c] Laboratory of Construction Materials, EPFL STI IMX LMC, Ecole Polytechnique Fédérale de Lausanne, 1015 Lausanne, Switzerland

ARTICLE INFO

Keywords:
Alkalis
Compressive strength
Humidity
Hydration

ABSTRACT

It has long been known that alkalis favor an increase in the early strength of cementitious materials but have a negative impact on long-term strengths. The reasons for the negative effect on later strengths are not clear. In this paper we investigated the influence of alkali addition on the properties of a white cement and for the first time propose a plausible mechanism for the late strength reduction. Quantitative XRD analysis and strength results showed that the addition of alkali generally limits the total degree of hydration (DoH) after 1 day. The evolution of internal relative humidity (RH) and saturated pore radius indicate that the more alkali added, the faster the decrease of internal RH and desaturation of the larger pores. The remaining solution in higher alkali system is concentrated in the smaller pores, where the needed supersaturation is higher. As a consequence, the hydration rate of cement is depressed by added alkali.

1. Introduction

The partial replacement of Portland cement by supplementary cementitious materials (SCMs) like calcined clay, fly ash or blast furnace slag is the most effective way to reduce CO_2 emissions of cementitious materials [1–4]. However, the levels of substitution are limited as the reaction of SCMs is slower than that of Portland cement phases, leading to a slower strength development at early age. An increase in the alkali content may be helpful to improve strength at early ages. For example, Fu et al. reported that the addition of 1 % Na_2SO_4 increased the strength of slag blended cement at 1 day by 43 %, from 5 MPa to 7.2 MPa [5]. Hanpongpun et al. used KOH to adjust the alkali content of LC^3–65 blended cement and found that the compressive strength at 1d was increased from 13 MPa to 16 MPa as the Na_2O_{eq} ($Na_2O_{eq} = Na_2O + 0.658{\cdot}K_2O$) was increased to 1.21 % [6].

The enhancement of early age strength by alkali can be attributed mainly to the accelerated reaction of the clinker phases especially alite. Kumar et al. simulated the alite hydration in solutions of various alkalinities (0.1 M ~ 0.5 M NaOH and KOH) and found that the increased pH leads to a faster rate of hydration and shorter duration of the induction, acceleration and deceleration regimes. Their simulation on the upturn in heat evolution rate affected by alkali showed that the precipitation of portlandite at the end of induction period occurred earlier, triggering the acceleration period, according to the solution controlled dissolution mechanism [7]. Mota Gasso et al. observed a similar acceleration of the hydration rate of alite by alkali, and found that the induction period almost disappeared in the system with 1.45 M of NaOH addition. The authors also pointed out the combined addition of alkali and gypsum further increase the DoH of alite after 10 h of hydration [8].

The merit of alkalis in improving the early age strength is offset by the fact that the strength at later ages is negatively affected. As early as 1968, Niel reported this reduction of later age strength by alkali in the 5th ICCC in Tokyo [9]. Later, Jawed and Skalny reviewed the work up to 1978 and concluded that high contents of alkali generally increase the early strength but decrease the final strength [10]. Smaoui et al. even reported a significant reduction in compressive and flexure strengths at all ages when the Na_2O_{eq} of concrete was above 1.25 % [11]. A recent study compared the alkali effect of 0.725 M Na_2SO_4 and 1.45 M NaOH on white Portland cement. The results showed that the addition of Na_2SO_4 can improve the 1d strength but then causes 12 % ~ 20 % of reduction in strength from 3d onwards, while for NaOH the strength was much lower at all ages compared to the system without alkali addition

* Correspondence to: F. Zunino, Physical Chemistry of Building Materials, Institute for Building Materials (IfB), ETH Zurich, CH-8093 Zurich, Switzerland.
** Corresponding author.
E-mail addresses: franco.zunino@ifb.baug.ethz.ch (F. Zunino), fzhwang@whut.edu.cn (F. Wang).

https://doi.org/10.1016/j.cemconres.2023.107348
Received 10 May 2023; Received in revised form 10 October 2023; Accepted 11 October 2023
Available online 14 October 2023

[12].

There is general consensus that the detrimental effect of alkalis on later age strength is related to higher porosity [11–15]. Many researchers argued that this increased porosity may be due to the changes in the morphology and composition of hydrates, especially C-S-H. Mori and coworkers [16] studied the influence of NaOH and Na_2SO_4 on the growth of C-S-H. NaOH resulted in a coarser C-S-H while the Na_2SO_4 favored acicular C-S-H. They suggested the differences in pore structure were related to alterations in the morphology of C-S-H. Mota Gasso et al. confirmed the changes of C-S-H by NaOH, which tended to have a lower Ca/Si ratio in the composition and be more foil-like in morphology. However, the authors also found that these differences in C-S-H did not to have a significant impact on the mechanical strength [8,12].

Changes in the morphology or composition of portlandite and aluminosilicate hydrates caused by alkalis have also been studied. By comparing the morphology of portlandite in plain and alkali added alite systems, Mota Gasso and coworkers reported the formation of more elongated and smaller crystals of portlandite in a system where Na_2SO_4 was added (the morphological alteration of CH in the presence of Na_2SO_4 could also be a consequence of high sulfate ion in the solution as reported by Galmarini et al. [17]). This phenomenon appeared to be more pronounced in the presence of NaOH, since NaOH drastically increase the supersaturations with respect to CH, leading to the very fast precipitation of CH close to alite surface. And this may even cause the change in the precipitation sequence that CH forms before any considerable amounts of C-S-H nucleates [8]. Li et al. [18] and Elakneswaran et al. [19] found that the U phase [$(CaO)_4(Al_2O_3)_{0.9}(SO_3)_{1.1}(-Na_2O)_{0.5}$:$16H_2O$] may form with high alkali concentrations, but no clear relationship between this U-phase and porosity or strength could be established. In summary the relation between strength and changes in hydrates caused by alkali is ambiguous and there are contradictory views in the literature.

The internal relative humidity (RH) has a strong influence on the hydration process [20,21], and it has been shown to affect the kinetics of hydration of blended cements in the long term [22]. The arising alkali content in the system increases the ions concentration in the pore solution, which leads to the suppression of RH due to the high ionic strengths and strong ionic interactions [13,21,23]. The present study looks at the evolution of microstructure and mechanical properties in systems with different amounts of alkali addition and considers the evolution of porosity and internal RH, which defines the fraction of pores that remain saturated. The development of compressive strength, degree of hydration, microstructure and porosity are also compared in the studied cement systems.

2. Materials and methods

2.1. Materials

A white Portland cement (WPC) (CEM I 52.5R) containing a low amount of alkali oxides was used in this study. The specific surface area of the WPC measured by nitrogen adsorption (BET model) was 1.4 m^2/g. The chemical (by XRF) and mineralogical (by XRD-Rietveld) composition of this white Portland cement is shown in Table 1. The particle size distribution of the WPC dispersed by isopropanol was measured by laser diffraction and is shown in Fig. 1. An extra 0.8 % of calcium sulphate dihydrate (gypsum) was added to adjust the sulfate balance in the WPC.

2.2. Experimental methods

2.2.1. Preparation of samples

NaOH pellets (>98 %, Reagent grade, Sigma-Aldrich) was used to adjust the alkali content of the systems studied. 30– 100 g of cement were mixed with deionized water or alkali solution, the water to cement ratio (w/c) was kept constant at 0.4. The cement pastes were mixed with a high shear mixer at 1600 rpm for 2 min. After that, the fresh pastes were directly tested or cast into plastic containers for hydration studies. The containers were sealed with parafilm and stored at 20 °C until the ages of interest. The details of the different pastes and nomenclature used in this paper are given in Table 2.

Table 1
Chemical (from XRF) and mineral (from XRD-Rietveld) composition of WPC.

Oxide	Percentage (%)	Anhydrous phase	Percentage (%)
SiO_2	24.41		
Al_2O_3	2.16		
Fe_2O_3	0.31	Alite	72.9
		C_2S	20.3
CaO	68.78	C_3A	3.2
MgO	0.63	Gypsum	1.7
		Bassanite	0.6
SO_3	2.04	Other	1.4
Na_2O	0.09		
K_2O	0.06		
Na_2O_{eq}	0.13		

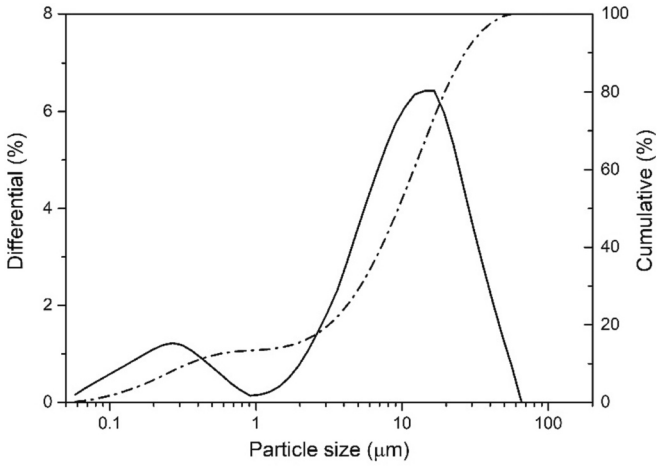

Fig. 1. Particle size distributions of WPC used in this study.

2.2.2. Compressive strength

Mortar samples were prepared following the EN 196-1 procedure but keeping the same w/c ratio (0.4) as the paste samples. For each system two stainless steel molds (160 × 40 × 40 mm) were used to prepare the required prisms for 1, 2, 3, 7 and 28 d strength tests. 3 prisms of 40 × 40 mm section were tested for compressive strength at each age and the error bars were taken as the standard deviation of the results.

2.2.3. X-ray diffraction (XRD)

XRD measurements were carried out on the freshly cut slices of hardened paste at 1, 2, 3, 7 and 28 days. The samples were measured in a Bragg-Brentano geometry in a PANalytical X'Pert Pro diffractometer equipped with a CuKα source operating at 45 KV and 40 mA. The 1/2° beam divergence slit was used and all the scans were measured from 7 to

Table 2
Recipes and nomenclatures of WPC systems.

Materials	Mixing solution	Total *Na_2O_{eq} in the system	Nomenclature in figures
WPC	Deionized water	0.13 %	0.13 % alkali
WPC	0.2 M NaOH	0.38 %	0.38 % alkali
WPC	0.4 M NaOH	0.63 %	0.63 % alkali
WPC	0.8 M NaOH	1.13 %	1.13 % alkali
WPC	1.6 M NaOH	2.13 %	2.13 % alkali

*$Na_2O_{eq} = Na_2O + 0.658 \cdot K_2O$.

70°2θ with a step size of 0.0167°2θ, which results in a total measurement time of about 14 min for each scan.

The commercial X'Pert HighScore Plus software (version 4.8) coupled with the ICCD database was used for calculating the total degree of hydration. The external standard method was selected to quantify the phase content by comparing the refined phase scale factor to that of a rutile (Kronos, 2300 Titanium dioxide) standard under identical measure conditions [24].

2.2.4. Mercury intrusion porosimetry (MIP)

A mercury intrusion porosimeter (Thermoscience, Pascal 140/440) was used to evaluate the porosity of paste samples at 1, 2, 3, 7 and 28 days. The hydration was stopped by immersing the samples in isopropanol (reagent grade, 99 % purity) at a volume ratio of solvent/sample of around 20 for 7 days. The samples were then stored in a desiccator for at least 2 days to evaporate the remaining isopropanol. Around 1 g of dried sample was placed in a glass dilatometer. A maximum pressure of 440 MPa was applied, sufficient for intrusion of down to pore entry radius of 2 nm, assuming a contact angle between the samples and mercury of 140°.

2.2.5. Scanning electron microscopy (SEM)

The microstructures were studied by BSE imaging using a FEI Quanta 200 SEM equipped with a 30mm^2 EDS detector (Bruker XFlash 4030) on polished sections of cement paste embedded in epoxy. The composition of inner C-S-H was obtained from the polished section of cement paste by point microanalyses (operating voltage 12 kV). The working distance was in all cases 12.5 mm. The spot size was adjusted to obtain a working current of about 0.9 nA, aimed to minimize the beam damage of the samples.

2.2.6. Relative humidity (RH)

After mixing, the fresh paste was quickly placed in a plastic vessel and then the internal RH was monitored by water activity probe HC2-AW-(USB) (Rotronic) in hermetic sample chambers. The sensors were calibrated before the experiments by using four different saturated salt solutions with an equilibrium RH from 75 % to 98 %. For each system, the evolution of internal RH was recorded up to 28 days and repeated three times.

To measure the RH of the pore solution, a hydraulic press up to 1500 MPa was first used to extract the pore solution from the samples at the ages of 1, 2, 3, 7 and 28 d. The pore solution obtained was tested by the same water activity probe as soon as possible to minimize the impact of reprecipitation. The measurement was following the same procedure as describe above and the RH value was read after reaching equilibrium (2 h in this paper). The measurement was repeated three times.

2.2.7. Calculation of saturated pore radius

When cement is hydrated under sealed and isothermal conditions, the chemical shrinkage of cement paste before setting leads to the reduction of bulk volume without generating internal pressure. After setting, a solid skeleton is formed inside the paste and the chemical shrinkage leads to the formation of gas filled voids in the larger pores (self-desiccation). The formation of menisci at the pore fluid-vapor interfaces results in the development of tensile stress in the pore fluid and the decrease in internal RH [25,26].

The RH_k related to the meniscus formation in a circular cylindrical pore can be described by the Kelvin - Laplace equation:

$$RH_k = exp\left(-\frac{2\gamma_s M_s cos\theta}{(r_p-\delta)\rho_s RT}\right) \quad (1)$$

where r_p is the pore radius, R is the universal gas constant (8.314 J/mol·K), T is the absolute temperature (in this paper, 293.15 K), γ_s is the surface tension of pore solution, M_s and ρ_s are the molar weight and density of pore solution, θ is the contact angle between liquid and solid. δ is the thickness of adsorbed liquid layer on the surface of the pores. Conventionally, the molar weight and density of the pore solution are assumed equal to those of pure water [25,26], leading to the M_s = 0.01802 Kg/mol and ρ_s = 1000 Kg/m^3. The γ_s of the pore solutions were measured by an optical tensiometer (Krüss Scientific) and the pendant drop method was applied on drops of 10 μL of size at 20 °C [27]. The γ_s of pure water measured by this method is 72.95 mN/m, and the measured values for the different pore solutions are given in Table 3.

The contact angle is assumed to be zero (i.e., perfect wetting conditions). δ is assumed usually to be below 1 nm and its value used in this paper was taken from [28], according to the different internal RH of studied systems, for example 0.8 nm for RH at around 90 %, 0.7 nm for RH at around 85 %.

The r_p, radius of the largest pore filled with pore solution (saturated pore) at the given RH_k is then defined by rearranging Eq. (1):

$$r_p = -\frac{2\gamma_s M_s}{ln(RH_k)\rho_s RT} + \delta \quad (2)$$

The drop of internal RH in cement paste depends on both the desiccation of pores (RH_k), and the water activity of pore solution (RH_S) [26]:

$$RH = RH_S \cdot RH_k \quad (3)$$

The r_p can be rewritten by combining Eqs. (2) and (3):

$$r_p = -\frac{2\gamma_s M_s}{ln\left(\frac{RH}{RH_s}\right)\rho_s RT} + \delta \quad (4)$$

the internal RH and RH_S can be directly measured by the water activity probes, and the values are then used to calculate the saturated pore radius.

3. Results and discussion

3.1. Mechanical properties

The development of compressive strength of WPC mortars with 0.13 % ~ 2.13 % alkali content are shown in Fig. 2. Compared to the 0.13 % alkali system, the presence of 0.38 % and 0.63 % alkali leads to a higher strength at early age, with an increase of 7.3 % and 12.4 % at 1d, respectively. After that, the strength in 0.38 % and 0.63 % alkali system develops slower, and is surpassed by that of 0.13 % alkali system at 3d and 2d, respectively. For mortars with 1.13 % and 2.13 % alkali content, the strength is always lower than that of 0.13 % alkali one. The presence of 2.13 % alkali leads to a maximum decrease of 35 % at 7 days.

From the above analysis, systems with low alkali addition such as 0.5 % (0.63 alkali system) have a positive influence on strength at early age but hinders the strength development at later age, while higher alkali addition (1 % and above) lower the strength at all studied ages. These results are in general agreement with previous observations reported in the literature.

3.2. Degree of hydration

Fig. 3 shows the influence of alkali content on the degree of hydration of WPC pastes. The increased alkalinity generally leads to a lower

Table 3
Surface tension of pore solution of each system.

Systems	Surface tension (mN/m)				
	1d	2d	3d	7d	28d
0.13 % alkali	69.7	70.4	69.8	70.1	69.4
0.63 % alkali	68.1	68.5	68.3	68.4	68.1
2.13 % alkali	64.0	63.9	63.9	64.1	64.0

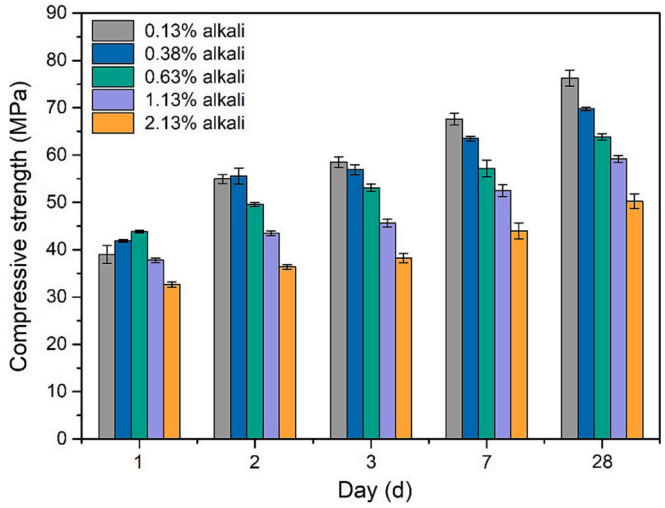

Fig. 2. Compressive strength results of white Portland cement mortars with different alkali content at w/c of 0.4 up to 28d.

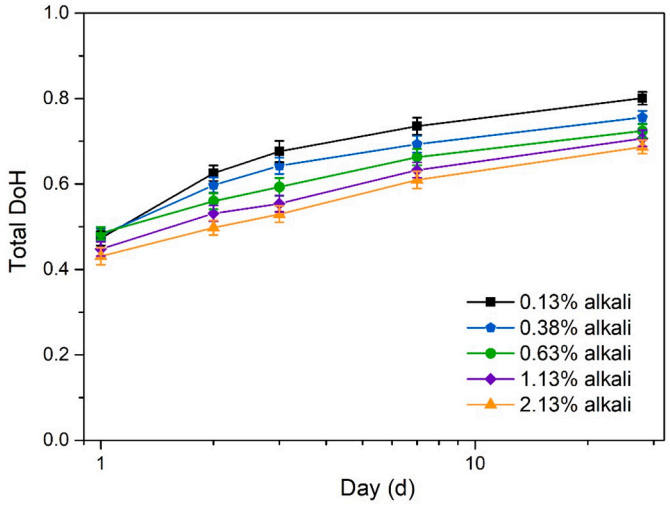

Fig. 3. Effect of alkali content on the total degree of hydration of white cement pastes at w/c of 0.4 up to 28 days.

DoH of WPC after 1 day, the higher the amount of alkali introduced, the lower the DoH obtained.

The compressive strengths as a function of DoH are shown in Fig. 4. Within the error of measurement, for the same DoH the strengths of alkali systems are roughly similar, except the 2.13 % alkali system where the strength is significantly lower at the same DoH.

3.3. Composition of C-S-H in WPC alkali systems

The influence of alkali content on the chemical composition of inner C-S-H at 28 days was investigated by the EDS point analysis (BSE images were shown in Fig. S1 in Supplementary materials). For each system, around 180 of points were collected on the inner C-S-H from different regions of the sample. Fig. 5a shows the Al/(Ca-S) against Si/(Ca-S) of these points, the increase in alkalinity has no significant effect on the alumina/calcium and silica/calcium ratio of C-S-H hydrates. In comparison, the incorporation of alkali in C-S-H is considerable promoted by the increasing alkalinity as shown in Fig. 5b. The average Na/(Ca-S) ratio in 2.13 % alkali system is >3 times that in 0.13 % alkali one, in agreement with other findings that sodium ion can be taken up in the interlayer space of C-S-H [29–32] or partially substitute calcium at the surface of C-S-H [33].

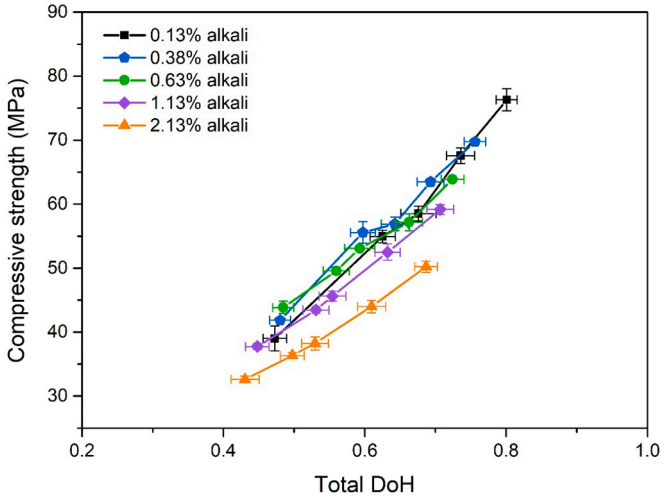

Fig. 4. Compressive strength of the white cement mortars versus total DoH of white cement paste at w/c of 0.4. The DoH of mortar is assumed to be the same with that of paste.

3.4. Relative humidity

Fig. 6a shows the evolution of internal RH up to 28d in white cement pastes with different alkali content. The increase of alkalinity clearly decreases the water activity in the pastes. However, this drop cannot only be attributed to changes in pore saturation, because the dissolved salts especially alkali ions in the pore solution also influence the internal RH. The RH of the expressed pore solutions is shown in Fig. 6b, the RH_s in 0.63 % and 2.13 % alkali systems are lower than the 0.13 % alkali system. Furthermore, in the same cement system the RH_s values at each age are roughly similar, which indicates that the alkali concentration in pore solution does not change significantly after 1d of hydration.

The RH_k related to the desiccation of pores is obtained by using Eq. (3) and the result is shown in Fig. 6c. As the drop due to dissolved salts in pore solution only have a minor effect on the overall internal RH (never higher than 4 %), the evolutions of RH_k have the similar tendency as total internal RH, where 2.13 % alkali system exhibits the strongest decrease in RH_k.

3.5. MIP and maximum saturated pore radius

Fig. 7 shows the pore volume measured by MIP of the 0.13 %, 0.63 % and 2.13 % alkali system at 1, 2, 3, 7 and 28 days. The radii of pores that remain saturated at the different ages were calculated by Eq. (4) and then marked on the MIP curves as the dash lines. From the MIP and RH results the total pore volume and the parts which are saturated and unsaturated is shown in Fig. 8.

At 1 day compared to 0.13 % alkali system, the extra addition of 0.5 % alkali slightly decreases the total pore volume, while 2 % alkali addition results in a higher pore volume (by 9.7 %). From then on, the pore volumes of 0.63 % and 2.13 % alkali systems are always larger than that of 0.13 % alkali system. The results are consistent with what is shown in Section 3.2 that the rise of alkalinity diminishes the total DoH quickly after 1 day, which leads to less amounts of hydrates to fill the pores.

The increased alkalinity results in faster desaturation of large pores compared to 0.13 % alkali system. At 1 day, the saturated pore radius in 0.13 % alkali and 0.63 % alkali cement paste is 104.5 nm and 89 nm respectively, while that in 2.13 % alkali paste is only 51.3 nm. The deposition of hydrate in these desaturated large pores will be much slower compared to saturated pores, likely taking place only in the film

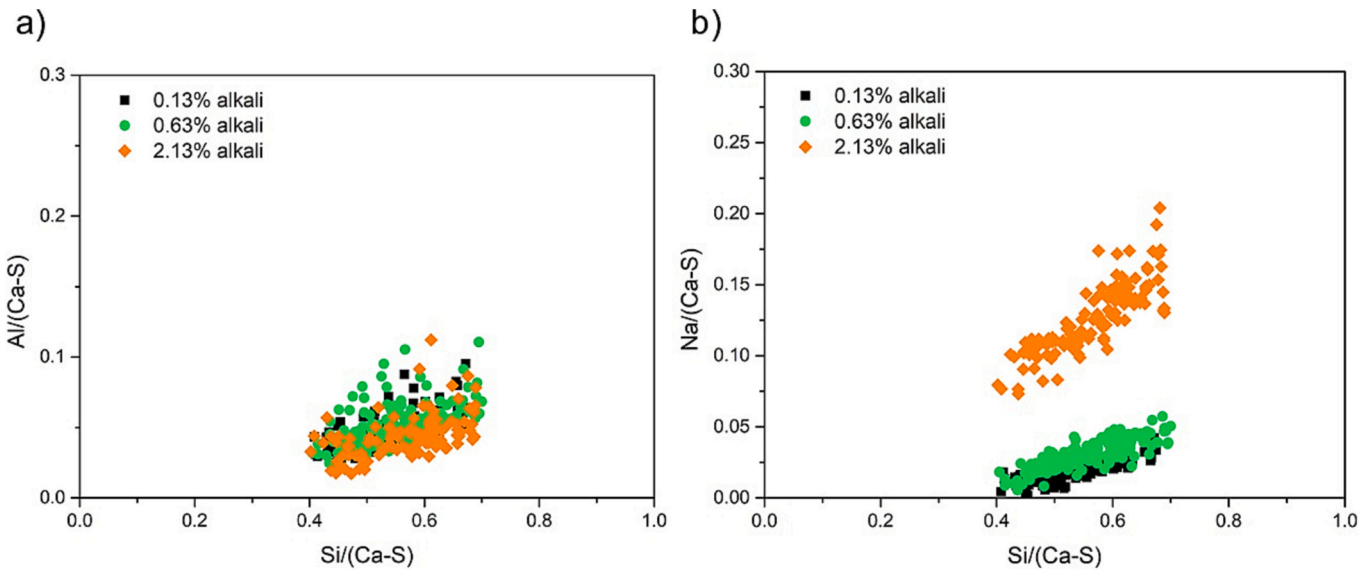

Fig. 5. Si/(Ca-S) vs Al/(Ca-S) (a) and Na/(Ca-S) (b) diagrams obtained from EDS point data collected from inner C-S-H of WPC systems at 28 days.

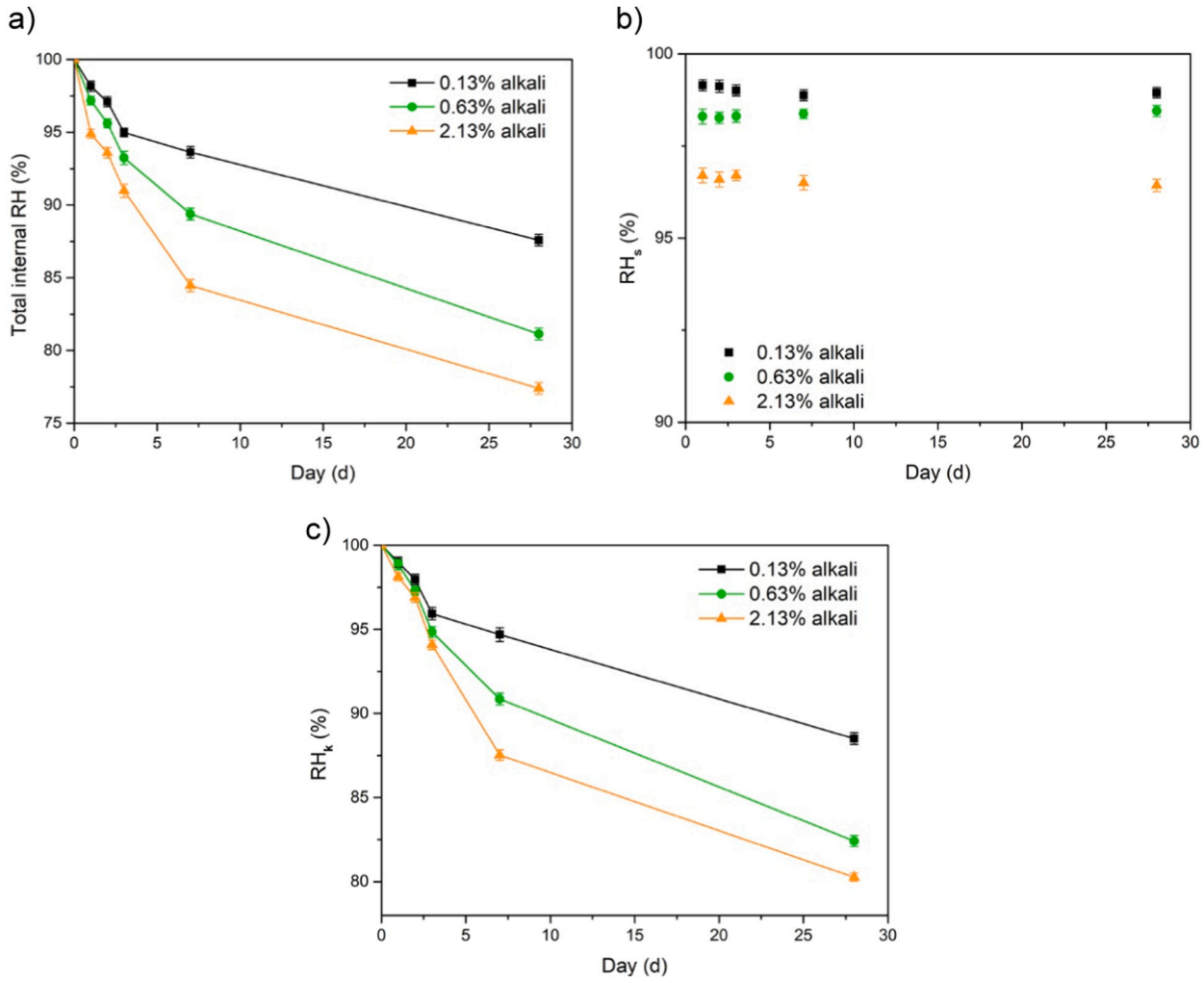

Fig. 6. Effect of alkali on the internal relative humidity (a), RH_s of pore solution (b) and RH_k related to the desiccation of pore (c) in white cement pastes up to 28 days of hydration.

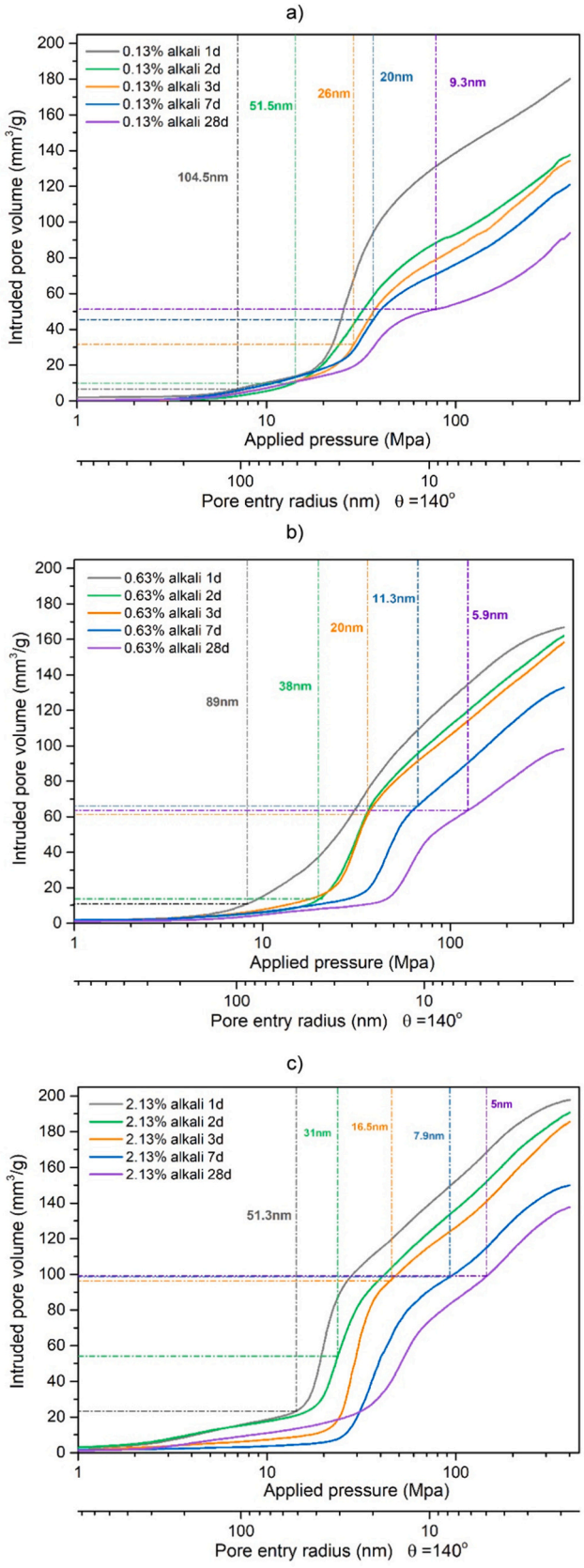

Fig. 7. The evolution of intruded pore volume up to 28 days in 0.13 % alkali (a), 0.63 % alkali (b), 2.13 % alkali (c) systems measured by MIP. The curves are plotted by pore volume versus applied pressure and pore entry radius as well. The saturated pore radius in each system at the corresponding days are marked as the dash lines.

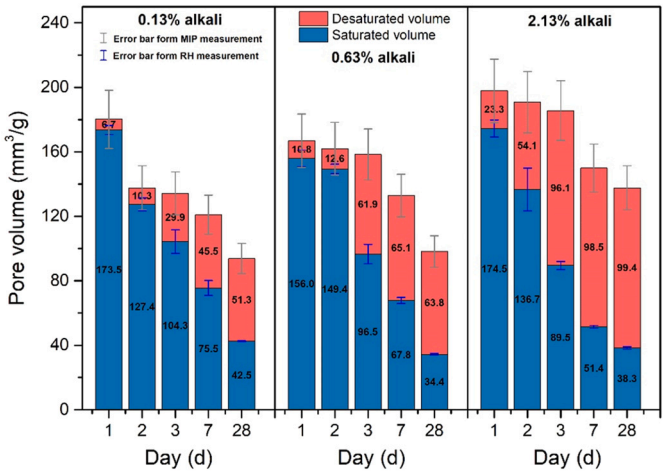

Fig. 8. Desaturated and saturated pore volume in 0.13 %, 0.63 % and 2.13 % alkali WPC systems up to 28 days.

of pore solution lining the inner surface of the pore [22]. The limiting saturated radius in each system continues to decrease from then on and reaches the values of 9.3, 5.9 and 5.0 nm respectively for the 0.13 %, 0.63 % and 2.13 % alkali systems at 28 days. Precipitation of hydrates occurs from solution, and requires supersaturation. The equilibrium saturation does not account for the surface energy of the crystal and this becomes larger as the curvature of the crystal increases [34–36]. Thus, the saturation needed for precipitation increases as the pore in which the crystal grows becomes smaller and the necessary curvature increases. In the 0.63 % and 2.13 % alkali systems effectively only pores of the size of the gel pores are still saturated at 28 days and hydration becomes very slow.

However, the decreased size of the saturated pores does not mean there is no remaining solution. As indicated in Fig. 8 the total volume of solution filled pore may even be slightly higher in the systems with higher alkali content (e.g., at 2 days).

3.6. Impact of pore size on hydration kinetics

The saturated volume in systems with high alkalinity is concentrated in smaller pores (e.g., pore radius below 5 nm in 2.13 % alkali system at 28 days). The energy barrier (supersaturation) for precipitating hydrates in these small pores is higher compared to the larger saturated pores available in the system with low alkali content. The required saturation index of C-S-H in 0.13 %, 0.63 % and 2.13 % alkali system for precipitating in different saturated pore radius can be approximated with Eq. (5) by considering the influence of both pore radius and relative humidity of pore solution of each system [37].

$$SI_{required} = \frac{2V_c \cdot \gamma_{CL}}{RTr_c} + \frac{V_C}{V_L} \cdot ln(RH_s) \quad (5)$$

Here, the V_c is molar volume of C-S-H, γ_{CL} is the interfacial energy between C-S-H and solution, V_L is molar volume of pore solution. The value of V_L is assumed equal to that of pure water (18 cm^3/mol), and the value of V_c and γ_{CL} are taken from [38,39], which is 75.63 cm^3/mol and 55 mJ/m^2, respectively (the parameters of used C-S-H solid solution model are shown in Table S1 in Supplementary materials). For 0.13 %, 0.63 % and 2.13 % alkali system the average value of RH_s from 1 to 28 days was used, which is 99 %, 98.3 % and 96.4 % respectively.

Due to the difficulty of precisely measuring the ion concentration of pore solution of system with high alkalinity, the average SI of C-S-H computed from pore solution of cement systems is taken from [37], which is 0.5. In the case of alkali systems, the referred study indicates that the SI of C-S-H in the pore solution increases with alkali concentration. Since no data on pore solution composition is available in this

study, a value of 0.5 was also assumed for alkali systems as it lies within the expected range of low and high alkali systems.

The minimum pore radius (from an SI perspective, providing a lower limit for the porosity where C-S-H can precipitate) of each system can be obtained from the crossover between the required SI curves and SI computed from pore solution, which is 5.2 nm in 2.13 % alkali system, 5.9 nm in 0.63 % alkali system and 6.25 nm in 0.13 % alkali system respectively, as shown in Fig. 9. While this approach is only semi-quantitative (given the assumption of the C-S-H SI values) this illustrates why precipitation of C-S-H slowdown in systems with alkali despite the presence of small saturated pores.

In Fig. 10 the pore sizes at which the SI needed for C-S-H precipitation is likely to be less than the SI of the pore solution is shown together with the maximum saturated radii (provides an upper limit above which precipitation is hindered) calculated from the MIP/RH data. This clearly indicates that the hydration will become slower due to the limited size of the saturated pores first for the 2.13 % alkali system and then for the 0.63 % alkali system while precipitation of hydrates should continue to be possible for the 0.13 % alkali system throughout the period of study. It must be stressed that there are several approximations in this calculation: the surface energy of C-S-H; the assumption of this surface energy as isotropic when C-S-H has a very anisotropic structure; and the assumption of the same composition of the pore solution for all systems. Nevertheless, it illustrates well how the lower RH in the systems with higher alkali content can limit the degree of hydration and therefore the strength development.

3.7. Discussion

The mechanism behind the decrease in strength development with the incorporation of alkalis at later ages has been debated for a long time. Most of the previous studies tried to find the answer by focusing the attention on the morphology and composition of hydrates affected by alkalis. However, these studies were unable to systematically explain the differences in performance observed in these systems [11,30,40,41]. Other studies found the strength is not affected by the morphological change of hydrates like C-S-H [8,12], highlighting the lack of overall consensus of the mechanisms involved. In this study, we illustrate how the lower RH in the systems with added alkali can affect the pores. As shown in Fig. 11, the pores in the systems with high alkali content are characterized by two features compared to that in the system with low alkali content: 1) more desaturated larger pores. Hydrates precipitation in those pores are very slow due to the lack of water; 2) plenty of saturated smaller pores. Hydrates deposition in those pores need a higher supersaturation. These two characteristics explain why added alkali slows down the rate of hydration and leads to lower strengths.

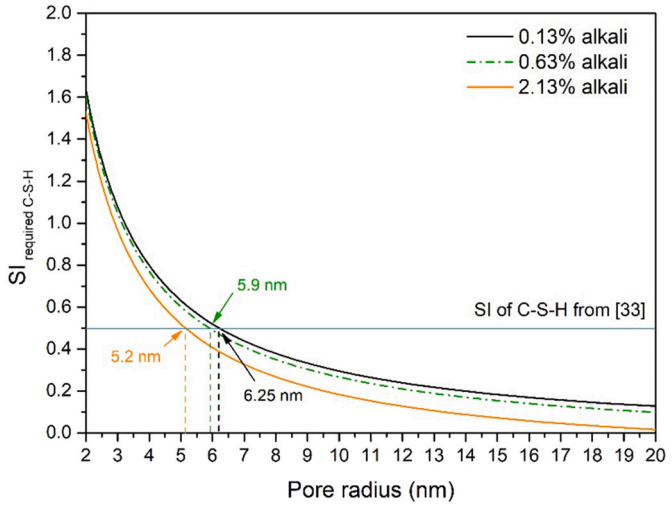

Fig. 9. Saturation index required for C-S-H precipitation in each system. The minimum pore radius for C-S-H precipitation in each system presences as the vertical dash line.

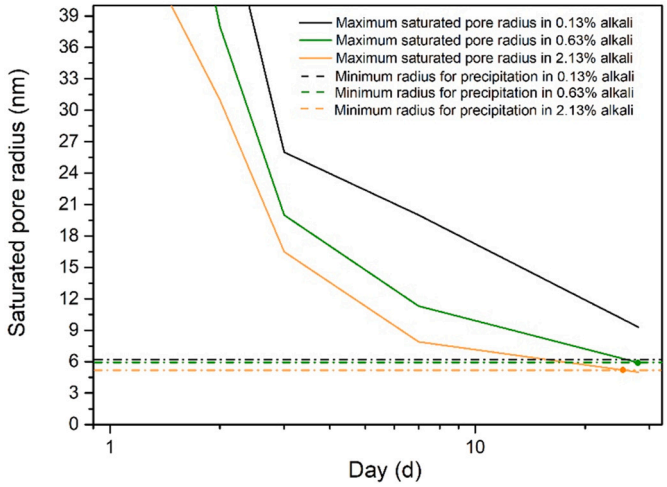

Fig. 10. Maximum saturated pore radius (from RH) and minimum pore radius for the precipitation of C-S-H (from SI) of each system.

It should be noted that the calculations including saturated pore radius (Fig. 7) and minimum pore radius for C-S-H precipitation (Fig. 10) are based on assumptions and can be influenced by the experiments error especially pore volume measured by MIP. To access the potential effect of these factors, a maximum 10 % deviation in the MIP data was taken and the deviation in RH was taken as the experimental error shown in Fig. 6c. This results in two error bars shown in the Fig. 8. It is very clear that these deviations do not reverse the fact that the system with high alkali content has more desaturated pore volume than the system with low alkali content, especially at the later hydration ages. Another aspect needs to be mentioned is the assumptions shown in Figs. 9 and 10, where the SI of C-S-H in the pore solution of all studied system was assumed to equal to 0.5. While the paper [37] indicates a higher supersaturation of the solution against the C-S-H phase in high alkali systems compared to low alkali systems. The suggested higher supersaturation can lead to the fact that higher alkali systems can still precipitate C-S-H in the smaller saturated pores for a longer period of time (longer than 28 days) as shown in Fig. S4 (Supplementary materials). However, even if this is true, it can't compensate the negative effect of massive desaturated larger pores on the hydration in high alkali system, otherwise the added alkali will lead to higher or at least similar strength at the later ages compared to the reference.

The rate limiting effects of the dissolution of clinker phases such as alite at the later ages, may play an important role in reducing the strength of high alkali systems, because there are more desaturated pore volumes in these systems that impede the movement of ions compared to low alkali system. Nevertheless, until more evidence of this phenomenon was presented in future studies, the proposed mechanism in the paper can well explain why added alkali can pose negative effect on the development of strength at the later hydration stage.

4. Conclusions

In this paper, various amounts of alkali were added to study their effects on the properties of white cement. The compressive strength, total degree of hydration and composition of C-S-H were compared in different WPC systems. The combination of porosity measured by MIP and saturated pore radius assessed by RH was performed to better illustrate how alkali deteriorate strength development at later age.

Based on the results presented, the following conclusions can be drawn:

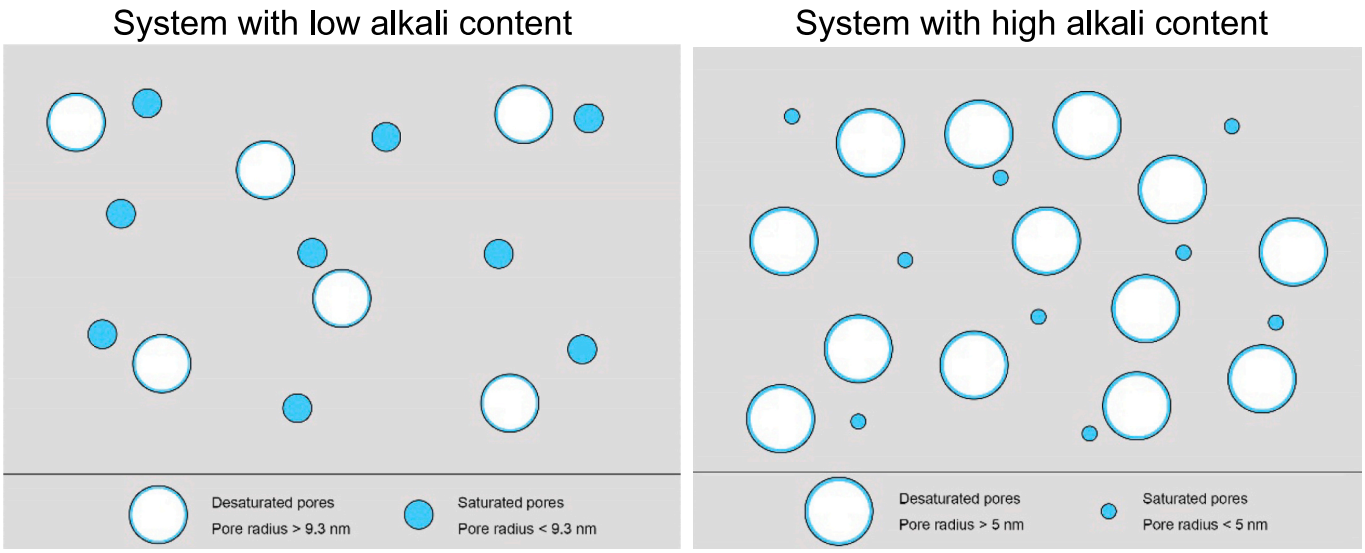

Fig. 11. The illustration of how added alkali influences the pores in the cement paste at 28 days.

1. The strength of all systems is proportional to the DoH of cement observed, except for the very high alkali addition, indicating no significant difference in the space filling capacity of the hydrates formed. The introduction of more alkali considerably promotes the uptake of alkali ions in the C-S-H hydrates, while the Ca/Al and Ca/Si ratios do not change significantly.
2. The internal relative humidity drops more and faster in the systems with added alkali, this leads to faster desaturation of the larger pores in which further hydrate growth is limited.
3. The fact that solution only remains in small pores slows the advancement of hydration, this results in lower DoHs for the systems with added alkali at later ages.
4. With low alkali addition, the strength is enhanced initially due to the acceleration of the hydration reaction, but this is quickly counterbalanced by the decrease in the size of pores still containing solution. High content of alkali addition is detrimental to the strength development at all ages.

CRediT authorship contribution statement

Mai Zhang: Conceptualization, Methodology, Experiments, Formal Analysis, Writing - original draft, Writing - review & editing. **Franco Zunino**: Conceptualization, Methodology, Discussion, review & editing. **Lu Yang**: Discussion, review & editing. **FaZhou Wang**: Discussion, review & editing, Supervision, Funding acquisition. **Karen Scrivener**: Conceptualization, Discussion, Supervision, review & editing.

Declaration of competing interest

The authors declare that they have no known competing financial interests or personal relationships that could have appeared to influence the work reported in this paper.

Data availability

Data will be made available on request.

Acknowledgement

The authors appreciate the financial supports from the National Natural Science Foundation of China under the contract (Nos. 51925205 and 52172025). The first author (Mai Zhang) would like to thank the financial supports from China Scholarship Council under the contract (No. 202106950023). The authors would like to thank Jinfeng Sun for helping the pore solution experiments and Qiao Wang for helping the MIP experiments.

Appendix A. Supplementary data

Supplementary data to this article can be found online at https://doi.org/10.1016/j.cemconres.2023.107348.

References

[1] K.M. Rahla, et al., Comparative sustainability assessment of binary blended concretes using Supplementary Cementitious Materials (SCMs) and Ordinary Portland Cement (OPC), J. Clean. Prod. 220 (2019) 445–459.
[2] K.L. Scrivener, et al., Eco-efficient cements: potential economically viable solutions for a low-CO2 cement-based materials industry, Cem. Concr. Res. 114 (2018) 2–26.
[3] Y. Zhang, et al., Effect of compressive strength and chloride diffusion on life cycle CO2 assessment of concrete containing supplementary cementitious materials, J. Clean. Prod. 218 (2019) 450–458.
[4] F. Zunino, et al., Limestone calcined clay cements (LC3), ACI Mater. J. 118 (2021).
[5] J. Fu, et al., Mechanisms of enhancement in early hydration by sodium sulfate in a slag-cement blend – insights from pore solution chemistry, Cem. Concr. Res. 135 (2020).
[6] W. Hanpongpun, K. Scrivener, The Effect of Alkali on the Properties of Limestone Calcined Clay Cement (LC3), Springer, Netherlands, Dordrecht, 2018, pp. 200–204.
[7] A. Kumar, et al., The influence of sodium and potassium hydroxide on alite hydration: experiments and simulations, Cem. Concr. Res. 42 (2012) 1513–1523.
[8] B. Mota, et al., The influence of sodium salts and gypsum on alite hydration, Cem. Concr. Res. 75 (2015) 53–65.
[9] E. Niel, The influence of alkali-carbonate on the hydration of cement, in: Proc. 5th Int. Cong. Chem. Cement. Tokyo, 1968, pp. 472–486.
[10] I. Jawed, J. Skalny, Alkalies in cement: a review. II. Effects of alkalies on hydration and performance of Portland cement, Cem. Concr. Res. 8 (1978) 37–51.
[11] N. Smaoui, et al., Effects of alkali addition on the mechanical properties and durability of concrete, Cem. Concr. Res. 35 (2005) 203–212.
[12] B. Mota, et al., Impact of NaOH and Na2SO4 on the kinetics and microstructural development of white cement hydration, Cem. Concr. Res. 108 (2018) 172–185.
[13] G. Sant, et al., The influence of sodium and potassium hydroxide on volume changes in cementitious materials, Cem. Concr. Res. 42 (2012) 1447–1455.
[14] Z. Li, et al., Effect of alkali content of cement on properties of high performance cementitious mortar, Constr. Build. Mater. 102 (2016) 631–639.
[15] A. Shayan, I. Ivanusec, Influence of NaOH on mechanical properties of cement paste and mortar with and without reactive aggregate, in: 8th Int. Conf. Alkali-Aggregate React, 1989, pp. 715–720.
[16] H. Mori, et al., The effect of alkali on the microstructure of hardened 3CaO·SiO2 paste, in: Proc. 25th Gen. Meet. Cem. Assoc. Japan, 1969, pp. 33–37.
[17] S. Galmarini, et al., Changes in portlandite morphology with solvent composition: atomistic simulations and experiment, Cem. Concr. Res. 41 (2011) 1330–1338.
[18] G. Li, et al., The U phase formation in cement-based systems containing high amounts of Na_2SO_4, Cem. Concr. Res. 26 (1996) 27–33.
[19] Y. Elakneswaran, et al., Durability of slag-blended cement due to U-phase instability in sulphate environment, Mater. Struct. 53 (2020).

[20] R.J. Flatt, et al., Why alite stops hydrating below 80% relative humidity, Cem. Concr. Res. 41 (2011) 987–992.
[21] M. Wyrzykowski, P. Lura, Effect of relative humidity decrease due to self-desiccation on the hydration kinetics of cement, Cem. Concr. Res. 85 (2016) 75–81.
[22] F. Zunino, K. Scrivener, Microstructural developments of limestone calcined clay cement (LC3) pastes after long-term (3 years) hydration, Cem. Concr. Res. 153 (2022).
[23] D. Ballekere Kumarappa, et al., Autogenous shrinkage of alkali activated slag mortars: basic mechanisms and mitigation methods, Cem. Concr. Res. 109 (2018) 1–9.
[24] S. R, Chapter 4. X-ray powder diffraction applied to cement, in: K.L. Scrivener, R. Snellings, B. Lothenbach (Eds.), A Practical Guide to Microstructural Analysis of Cementitious Materials, 2015.
[25] L. Pietro, et al., Autogenous shrinkage in high-performance cement paste: an evaluation of basic mechanisms, Cem. Concr. Res. 33 (2003) 223–232.
[26] Z. Hu, et al., A novel method to predict internal relative humidity in cementitious materials by 1 H NMR, Cem. Concr. Res. 104 (2018) 80–93.
[27] T. Soori, et al., A machine learning approach for estimating surface tension based on pendant drop images, Fluid Phase Equilib. 538 (2021).
[28] R. Badmann, et al., The statistical thickness and the chemical potential of adsorbed water films, J. Colloid Interface Sci. 82 (1981) 534–542.
[29] S. Hong, F.P. Glasser, Alkali sorption by C-S-H and C-A-S-H gels: part II. Role of alumina, Cem. Concr. Res. 32 (2002) 1101–1111.
[30] S. Hong, F.P. Glasser, Alkali binding in cement pastes: part I. The C-S-H phase, Cem. Concr. Res. 29 (1999) 1893–1903.
[31] B. Lothenbach, A. Nonat, Calcium silicate hydrates: solid and liquid phase composition, Cem. Concr. Res. 78 (2015) 57–70.
[32] E. L'Hôpital, et al., Alkali uptake in calcium alumina silicate hydrate (C-A-S-H), Cem. Concr. Res. 85 (2016) 122–136.
[33] B. Jönsson, et al., Controlling the cohesion of cement paste, Langmuir 21 (2005) 9211–9221.
[34] G.W. Scherer, Stress from crystallization of salt, Cem. Concr. Res. 34 (2004) 1613–1624.
[35] G.W. Scherer, Crystallization in pores, Cem. Concr. Res. 29 (1999) 1347–1358.
[36] K. Scrivener, et al., Advances in understanding cement hydration mechanisms, Cem. Concr. Res. 124 (2019).
[37] M. Zajac, et al., Late hydration kinetics: indications from thermodynamic analysis of pore solution data, Cem. Concr. Res. 129 (2020).
[38] D.A. Kulik, Improving the structural consistency of C-S-H solid solution thermodynamic models, Cem. Concr. Res. 41 (2011) 477–495.
[39] M.R. Andalibi, et al., On the mesoscale mechanism of synthetic calcium–silicate–hydrate precipitation: a population balance modeling approach, J. Mater. Chem. A 6 (2018) 363–373.
[40] D.P. Bentz, Influence of alkalis on porosity percolation in hydrating cement pastes, Cem. Concr. Res. 28 (2006) 427–431.
[41] W. Chen, H.J.H. Brouwers, Alkali binding in hydrated Portland cement paste, Cem. Concr. Res. 40 (2010) 716–722.